TITLE: Recombinant expression in E. coli of human FGFR2 with its transmembrane and extracellular domains

Authors: Adam Bajinting[1,2], Ho Leung Ng[1,3]

[1]University of Hawaii at Manoa, Department of Chemistry

[2]St. Louis University School of Medicine

[3]University of Hawaii Cancer Center

Corresponding author: Ho Leung Ng, hng@hawaii.edu

ABSTRACT

Fibroblast growth factor receptors (FGFRs) are a family of receptor tyrosine kinases containing three domains: an extracellular receptor domain, a single transmembrane helix, and an intracellular tyrosine kinase domain. FGFRs are activated by fibroblast growth factors (FGFs) as part of complex signal transduction cascades regulating angiogenesis, skeletal formation, cell differentiation, proliferation, cell survival, and cancer. We have developed the first recombinant expression system in E. coli to produce a construct of human FGFR2 containing its transmembrane and extracellular receptor domains. We demonstrate that the expressed construct is functional in binding heparin and dimerizing. Size exclusion chromatography demonstrates that the purified FGFR2 does not form a complex with FGF1 or adopts an inactive dimer conformation. Progress towards the successful recombinant production of intact FGFRs will facilitate further biochemical experiments and structure determination that will provide insight into how extracellular FGF binding activates intracellular kinase activity.

Keywords: FGFR, fibroblast growth factor receptor, membrane protein expression, receptor tyrosine kinases, FGF, FGFR2

INTRODUCTION

As receptor tyrosine kinases (RTKs), FGFRs have three primary domains: an extracellular domain (ECD), a single transmembrane helix (TM), and an intracellular tyrosine kinase domain (KD) (**Fig. 1**). These proteins are expressed primarily in endothelial, fibroblast, vascular smooth muscle, neuroectodermal, and mesenchymal cells. When activated by fibroblast growth factors (FGFs), these receptors are responsible for activating mechanisms via trans-autophosphorylation that result in angiogenesis, skeletal formation, and cell differentiation, proliferation, survival, and growth. Within the subfamily are four types of FGFRs: FGFR1, FGFR2, FGFR3, and FGFR4, which share 55-72% sequence homology. Due to their critical roles in cell and tissue development, mutations of FGFRs are known to lead to achondroplasia (poor cartilage growth) and developmental disorders that exhibit craniosynostosis (improper skull formation) (Turner & Grose, 2010). FGFR2 and FGFR3 have also been implicated in cancers such as bladder cancer, and inhibitors are being investigated as potential cancer therapeutics (Turner & Grose, 2010; Brooks, Kilgour & Smith, 2012; Daniele et al., 2012; Dieci et al., 2013).

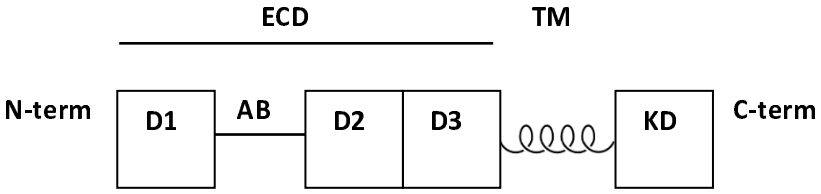

Fig. 1. **Schematic of domains and motifs in FGFR2.** D1-D3 are the immunoglobulin domains. AB is the acid box motif. ECD is the extracellular domain (or ectodomain). TM is the single transmembrane helix. KD is the intracellular kinase domain.

Crystal structures have been determined of the ectodomains and kinase domains of the FGFRs (Mohammadi, Schlessinger & Hubbard, 1996; Plotnikov et al., 1999, 2000; Schlessinger et al., 2000; Yeh et al., 2002; Zhang et al., 2009). The ectodomain is composed of three immunoglobulin (Ig) domains termed D1, D2, and D3. Between D1 and D2 is an acid box motif, a sequence of 20 acid-rich amino acids that binds to divalent cations to stabilize the interaction between FGFR and heparin/heparin sulfate proteoglycans (HSPGs) (Patstone & Maher, 1996). The acid box also mediates interactions with other proteins (Sanchez-Heras et al., 2006, p.) and plays a key role in auto-inhibition (Kalinina et al., 2012). For the FGFR2 ECD+TM construct in particular, the structure of the ECD lacks both the acid box and the D3 domain. Removal of both regions increases the affinity for heparin and the ability of FGF to active FGFR (Wang et al., 1995). The D3 domain is unnecessary for FGF1 activation and is involved in differential responses to different FGFs (Yu et al., 2000).

There are many open questions about the structure of FGFRs regarding the transmembrane helix and how it connects the ECD and KD. There is an NMR structure of the FGFR3 TM that shows it as a single alpha helix (Bocharov et al., 2013). However, the biological relevance of this structure is unclear as the data was collected from a construct containing only the TM and the extracellular juxtamembrane region, without the ECD or KD. As the TM represents a tiny proportion of the full-length FGFR, it is likely that the natural conformation of the TM in the intact receptor in vivo differs significantly from the isolated peptide.

X-ray crystallography of a multi-domain construct containing the TM would provide more insight into the receptor activation mechanism and how activation status is transduced across the membrane. Bocharov et al. proposed a "string puppet theory" mechanism of signal transduction based on the NMR structure of the TM helix (Bocharov et al., 2013). The string puppet theory proposes that FGFR dimerizes in an inactive form via its transmembrane domains without FGF and heparin; the active conformation results when the inactive dimer binds to FGFs. Details of the stoichiometry of FGF, heparin, and FGFR in the activated complex are also debated (Lemmon & Schlessinger, 2010). The strongest data supporting or invalidating hypotheses about inactive and active FGFR states will come from detailed structures of intact FGFR.

Here we describe our development of a recombinant expression system in E. coli to produce significant quantities of functional FGFR with its TM linked to either its ECD or KD for eventual structural studies. While we were not able to express the intact FGFR, we successfully expressed constructs of FGFR2 and FGFR3 containing ECD+TM and TM+KD. We show that the FGFR2 ECD+TM construct is functional in binding heparin and dimerizing. Our simple recombinant method will facilitate biochemical experiments studying the relationship between the TM and other domains.

MATERIALS & METHODS

DNA cloning of constructs

PIPE (polymerase incomplete primer extension) cloning was used to obtain specific domain combinations of FGFR2, and the cloning vector pSpeedET with an N-terminal E. coli

maltose binding protein (MBP) fusion tag of 42.5 kDa (Klock & Lesley, 2009). The domain combinations created are shown in Table 1. The FGFR inserts were amplified by PCR using Phusion Hi Fidelity DNA Polymerase, 200 mM dNTP, 0.5 μM forward and reverse primers, and 6% DMSO. PCR products were extracted from agarose gel and purified using Thermo Scientific GeneJet Gel Extraction Kits. The MBP fusion tag was added to the construct to improve construct solubility and expression (Kapust & Waugh, 1999), allow purification by amylose affinity chromatography, and identification by Western blot with an anti-MBP antibody (New England Biolabs (E-8038)). Cloning results were confirmed by DNA sequencing.

Table 1. FGFR2 and FGFR3 constructs created

Construct	Expected Size (kDa)
MBP + FGFR2 31-406 (ECD + TM)	71.5
MBP + FGFR2 370-651 (TM + KD)	73.7
MBP + FGFR2 31-651 (ECD + TM + KD)	111.5
MBP + FGFR3 143-405 (ECD + TM)	71.3
MBP + FGFR3 365-771 (TM + KD)	87.9
MBP + FGFR3 143-771 (ECD + TM + KD)	112.3

Small scale expression

Small scale expression studies were performed using *E. coli* Lemo21 cells (New England Biolabs). 10 mL inoculate from an overnight culture was added to 100 mL of TB media and

shaken at 37° C. The OD_{600} was monitored as it approached an absorbance of 0.6. Once the culture reached an OD_{600} of 0.4-0.5, the cells were cooled to 18° C in the shaker to slow the growth of cells. Once it reached OD of 0.6, 1 mL of each construct culture was taken to serve as a negative control for later experiments. Isopropyl β-D-1-thiogalactopyranoside (IPTG) was then added at a 0.1mM final concentration to each culture to induce expression. The cells were then grown in a shaker at 18° C overnight.

Harvesting and lysing cells

Each of the cultures was centrifuged at 4° C at 4,700 rpm for 10 minutes. The culture media was discarded, and the pellet was washed by resuspending in lysis buffer (300 mM NaCl, 50 mM HEPES at pH 7.5, 0.1 mM $MgSO_4$, 5% glycerol, 0.5 mM TCEP, benzamidine, and PMSF). It was centrifuged at 4,700 rpm for 10 minutes, after which, the lysis buffer was discarded. 20 mg of post induction E. coli cell pellet was resuspended in 180 µL of lysis buffer (300 mM NaCl, 50 mM HEPES at pH7.5, 0.1 mM $MgSO_4$, 5% glycerol, 0.5 mM TCEP, benzamidine, and PMSF). 20 µL of 10 mg/mL lysozyme stock was added in addition to 0.3 µL of DNAse I. Next, the lysis reaction was put through three freeze-thaw cycles to lyse the cells.

Western blot analysis

Western blotting was performed on PVDF membranes after wet transfer from polyacrylamide gels. Membranes were blocked with Amresco RapidBlock solution for 5 minutes and then incubated with HRP-conjugated anti-MBP monoclonal antibody (New England Biolabs) overnight at 4° C. Membranes were then washed three times for 5 minutes with 20 mM

Tris-HCl pH 7.5, 150 mM NaCl, and 0.1% Tween 20. Finally, the blots were developed using the KPL TMB Membrane Peroxidase Substrate System kit.

Large-scale expression studies

Once the two best candidates for continued expression studies were determined, the FGFR2 ECD+TM constructs were expressed at a larger scale. The expression procedures (transformation and inoculation) are identical except that instead of 10 mL of initial culture (in LB) to inoculate 100 mL of TB, 100 mL of initial culture was grown and inoculated into 1000 mL of TB.

Once the culture reached OD_{600} of 0.4-0.5, the cells were cooled to 18° C in the shaker to slow growth. Isopropyl β-D-1-thiogalactopyranoside (IPTG) was then added at 0.1 mM final concentration to induce expression.

Cell lysis

Each construct's cell pellet was resuspended in lysis buffer by vortexing and physically mixing with a pipet to ensure homogeneity. 1 µL of DNAse I was added in addition to 1 µM final concentration of $CaCl_2$, and additional protease inhibitors (E-64, pepstatin, and bestatin) prior to lysis by sonication at 4° C. Sonication was performed for a total of 2 minutes, divided into 20 seconds of sonication followed by 40 seconds of rest. Following sonication, the suspensions were centrifuged at 20,000 rpm using a JA20 rotor for 30 minutes.

Detergent extraction of FGFR from cell membranes

Unlike the small-scale expression trials, large-scale expression studies included detergent extraction of FGFR2 from cell membranes. For every 100 µg of cell pellet or 100 µL of supernatant, 500 µL of lysis buffer with 1% detergent solution was added and resuspended in the presence of PMSF. The suspension for each was then constantly inverted for 2 hours at 25° C. The suspensions were then centrifuged at 14,000 rpm. Both pellet and supernatant were then stored at -80° C. Several detergents were tested for optimal extraction from the cell pellet and the supernatant from the centrifugation: 1% n-dodecyl-β-D-maltopyranoside (DDM), 1% Brij 35, and 1% Brij 58 for the samples of pellet and supernatant. FGFR2/3 constructs were tested for binding to MBPTrap HP affinity chromatography resin (GE Healthcare).

Refolding by dialysis

Both FGFR2 and FGFR3 constructs containing ECD+TM were refolded by dialysis as described previously (Mohammadi, Schlessinger & Hubbard, 1996). The cell pellets were washed and resuspended with 0.5% guanidinium-HCl and centrifuged at 45,000g for 20 minutes. Next, the pellets were solubilized in dialysis solution #1 (6 M guanidinium-HCl, 0.1% DDM, 10 mM DTT, and protease inhibitors E-64, benzamidine, PMSF, bestatin, and pepstatin at a pH of 8.0). To facilitate solubilization, the cell pellet and dialysis solution mixture was warmed briefly to 40° C followed by vortexing at room temperature. The total mixture was about 13 mL. All 13 mL of the solubilized inclusion bodies in the dialysis solution #1 was loaded into a dialysis membrane. This was placed in a beaker with 700 mL of dialysis solution #2 (25 mM HEPES, 150 mM NaCl, 10% glycerol, and 1 mM L-cysteine at pH 7.5) at 4° C overnight with constant stirring using a magnetic stir bar. After 19 hours, the sample within the dialysis membrane was then centrifuged at 24,000g for 30 minutes and the supernatant was stored at -80° C.

FGF1 expression and purification

The FGF1 gene with an N-terminal His-tag in the expression vector pMCSG7 was obtained from the DNASU Plasmid Repository at Arizona State University. FGF1 was first purified using a 1 mL HiTrap GE Healthcare heparin affinity chromatography column, using elution buffer containing 1 M NaCl, 10% glycerol, 25 mM HEPES, 10 mM imidazole, and benzamidine with a pH of 7.5, as described previously (Pellegrini et al., 2000).

Determination of success was purification by heparin affinity chromatography was by SDS-PAGE and Western blot analysis, but instead of using an anti-MBP antibody (HRP conjugated), an anti-His antibody (HRP conjugated) from Pierce was used. This was then followed by size exclusion chromatography. The running buffer used for size exclusion chromatography (SEC) was 25 mM HEPES, 0.1% DDM, and 150 mM NaCl.

Initial functionality test of FGFR2

The first step in testing functionality is to determine whether FGFR2 can bind to heparin and FGF1. The 1 mL HiTrap Heparin Affinity Chromatography (GE Healthcare) column was used to test for heparin binding. First, 10 column volumes (CVs) of binding buffer (150 mM NaCl, 25 mM HEPES pH 7.5, benzamidine, and 0.1% DDM) was loaded onto the column with a syringe to equilibrate the column. Next 1 mL of FGF1's elution from SEC was loaded onto the column followed by 10 CVs of binding buffer. This was then followed by FGFR2's supernatant from the dialysis. Following loading, FGFR2 was washing with 5 CVs of binding buffer. This was then followed by running 10 CVs of elution buffer (25 mM HEPES pH 7.5, 1.5 M NaCl, 0.1% DDM, benzamidine, and PMSF).

This was followed by SDS-PAGE and western blot analysis. The anti-MBP antibody was used to detect FGFR2, and the anti-His-tag antibody was used to detect FGF1. Heparin affinity purification was followed by size exclusion chromatography.

RESULTS

Small scale expression of FGFR2 and FGFR3 constructs

We performed small-scale expression trials of the FGFR2 and FGFR3 constructs. The western blot with an anti-MBP antibody showed significant quantities of FGFR2 and FGFR3 ECD+TM in both the soluble and cell pellet fractions (**Fig. 2**). The intact receptors were not detected. FGFR2 TM+KD was not detected, but FGFR3 TM+KD was found in the cell pellet fraction. We considered the FGFR2 and FGFR3 ECD+TM constructs to be the most promising for larger scale expression studies. In addition, for most of the constructs, prominent bands corresponding to the molecular weight of MBP were observed suggesting significant proteolysis of the fusion protein.

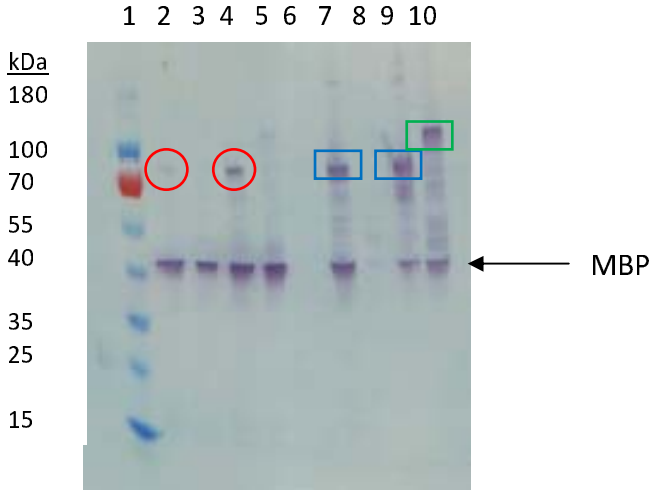

Fig. 2. Western blot analysis of small scale expression of FGFR2 and FGFR3 constructs using anti-MBP antibody. Lane 1: Ladder. Lane 2: FGFR2 31-406 from supernatant. Lane 3: FGFR2 370-651 from supernatant. Lane 4: FGFR3 143-405 from supernatant. Lane 5: FGFR 3:

365-771 from supernatant. Lane 6: Skip, Lane 7: FGFR2 31- 406 from pellet. Lane 8: FGFR2 370-651 from pellet. Lane 9: FGFR3 143-405 from pellet. Lane 10: FGFR3 365-771 from pellet. Circled in red are bands consistent with FGFR2 and FGFR3 ECD+TM from supernatant. Boxed in blue are bands consistent with FGFR 2 and 3 ECD+TM from the cell pellet fraction. Boxed in green is a band consistent with FGFR3 TM+KD from the cell pellet fraction.

Large-scale expression studies and detergent extraction analysis

We performed expression trials of the FGFR2 and FGFR3 ECD+TM constructs in larger scale, 1L cultures. We tested three detergent solutions, containing 1% DDM, Brij 35, or Brij 58 for extraction of FGFR2/3. The western blot with an anti-MBP antibody on the detergent-extracted fractions showed significant quantities of FGFR2 and FGFR3 ECD+TM from both the soluble and cell pellet fractions (**Fig. 3**). We determined that DDM, Brij 35, and Brij 58 extracted FGFR2/3 similarly well. We decided to use DDM for all following procedures because it is the most commonly used detergent for membrane protein crystallography (Privé, 2007; Loll, 2014). As in the small scale expression trials, we observed prominent bands corresponding to proteolyzed MBP. Due to the large amounts of protein loaded, we also observed high amounts of non-specific binding in the western blot. We also observed a high molecular weight band that comigrated near the 180 kDa ladder band that we tentatively identify as oligomerized or aggregated FGFR2/3.

Based on the high expression levels shown on this western blot, especially from the soluble fraction, we initially decided FGFR3 ECD+TM would be our lead candidate for further expression and purification studies. However, we found that FGFR3 from the soluble fraction did not bind to the MBP affinity column. This suggested that the fusion protein, MBP-FGFR3, was folded incorrectly. Thus, we refocused efforts on FGFR2. We pursued expression of FGFR2 ECD+TM in inclusion bodies and refolding by dialysis, as demonstrated previously for FGFR2

ECD (Mohammadi, Schlessinger & Hubbard, 1996). Refolding provided high yields of FGFR2 ECD+TM, > 4 mg from 1 L of culture.

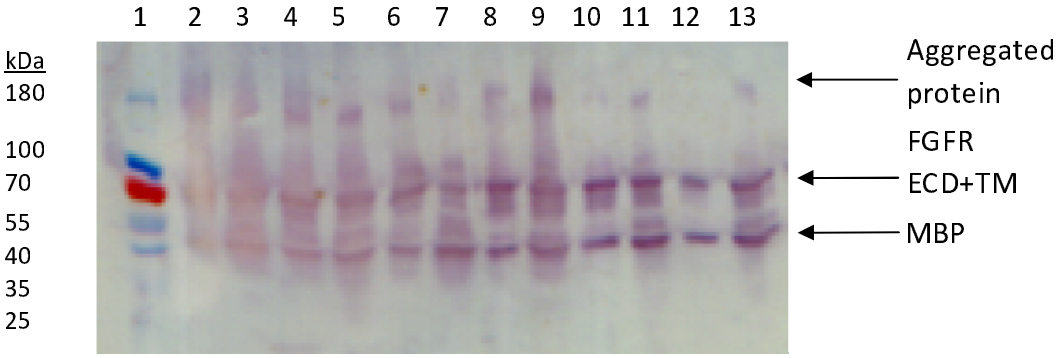

Fig. 3. Western blot of detergent extractions of large-scale expression constructs FGFR2 and FGFR3 ECD+TM. Lane 1: Ladder. Lane 2: FGFR2 pellet with 1% DDM. Lane 3: FGFR 2 supernatant with 1% DDM. Lane 4: FGFR2 pellet with 1% Brij 35. Lane 5: FGFR2 supernatant with 1% Brij 35. Lane 6: FGFR2 pellet with 1% Brij 58. Lane 7: FGFR2 supernatant with 1% Brij 58. Lane 8: FGFR3 pellet with 1% DDM. Lane 9: FGFR3 supernatant with 1% DDM. Lane 10: FGFR3 pellet with 1% Brij 35. Lane 11: FGFR3 supernatant with Brij 35. Lane 12: FGFR3 pellet with 1% Brij 58. Lane 13: FGFR3 supernatant with 1% Brij 58.

Binding of refolded FGFR2 to heparin

To test that the refolded FGFR2 ECD+TM retained its function, we sought to determine whether it was able to 1) bind heparin, 2) bind FGF1, and 3) dimerize. We tested the refolded fraction for binding to a heparin affinity chromatography column. A western blot with an anti-MBP antibody of the eluted fractions from the heparin affinity column demonstrated the presence of MBP-FGFR2 ECD+TM, supporting that the refolded FGFR2 bound heparin (**Fig. 4**).

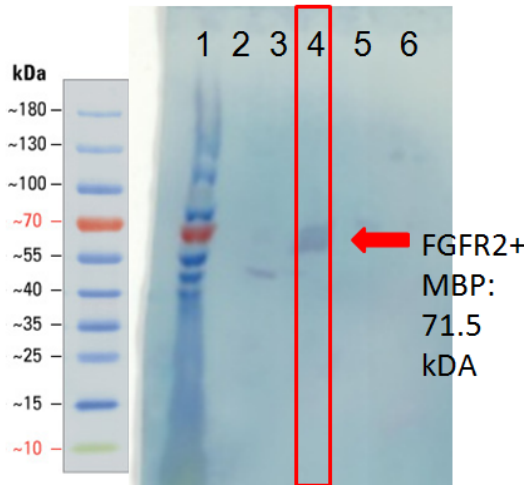

Fig. 4. Western blot of heparin affinity column purification fractions using anti-MBP antibody. Lane 1: ladder. Lanes 2-3: wash fractions. Lanes 4-6: elution fractions.

Refolded FGFR2 forms dimers but does not bind FGF1

The main elution fraction from the heparin affinity purification was then passed through a size exclusion chromatography column to resolve its components (**Fig. 5**). The first peak, eluting at 25.76 mL, corresponds to a molecular weight of 200 kDa. The second peak, eluting at 30.79 mL, corresponds to between 66 and 79 kDa. The third primary peak, eluting at 34.99 mL, corresponds to a size between 12 and 20 kDa. Each of these three primary peaks was analyzed by SDS-PAGE and western blots (**Fig. 6**). The second peak corresponded to the molecular weight of the MBP-FGFR2 ECD+TM construct (71.5 kDa) and was identified by western blot with an anti-MBP antibody (data not shown). The third peak corresponded to FGF1 from its molecular weight (17.5 kDa) and was identified by western blot with an anti-His-tag antibody (data not shown).

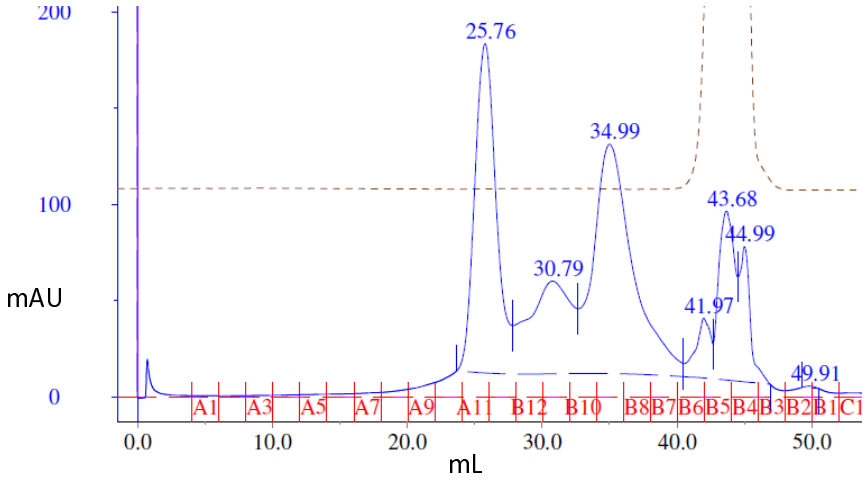

Fig. 5. Size exclusion chromatography of the main heparin affinity elution fraction. Elution fractions are marked in red.

We considered two possibilities for the identity of the first peak: 1) a complex of MBP-FGFR2 dimer with FGF1, 2) a dimer of MBP-FGFR2 in DDM micelles. Western blot analysis with an anti-MBP antibody confirmed the presence of MBP-FGFR2 ECD+TM (**Fig. 6**). We eliminated the possibility of the peaking being the FGFR2-FGF1 complex because the expected molecular weight is 230.5 kDa, and western blot analysis with an anti-His-tag antibody did not show the presence of FGF1 (data not shown). In contrast, the expected molecular weight of an MBP-FGFR ECD-TM dimer with a DDM micelle is 213 kDa. Potentially, the inclusion of the TM region or DDM may stabilize an inactive conformation of the dimer not capable of binding FGF1.

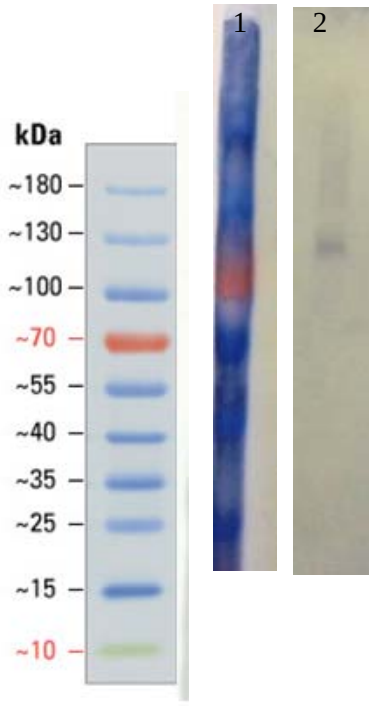

Fig. 6. Western blot of the first peak from SEC using anti-MBP antibody. Arrow points to band correlating to FGFR2 construct size (71.5kDa). Lane 1: Ladder. Lane 2: SEC fraction A12. Both lanes are cropped from the same blot.

CONCLUSIONS

Our results support the possibility of expressing mostly functional FGFR2 ECD+TM in E. coli. Key steps include the use of the Lemo 21 (DE3) strain, refolding from inclusion bodies, and use of the detergent DDM throughout all extraction and purification procedures. The purified FGFR2 ECD+TM demonstrated the ability to dimerize and bind heparin but did not form a stable complex with FGF1 as observed by size exclusion chromatography. This may suggest that the purified FGFR2 was not fully folded or functional. Other possible explanations include 1) inclusion of the TM or detergent favors an inactive conformation or 2) stable complex formation requires the addition of accessory molecules such as heparin, heparan sulfate, or sodium octasulfate (Zhang et al., 2009). The potential inhibitory role of the TM merits further investigation.

Funding

This project was funded by NSF CAREER Award 1350555 (H.L.N.), the University of Hawaii at Manoa, and the University of Hawaii at Manoa Undergraduate Research Opportunities Program (A.B).

Competing interests

The authors declare no conflict of interest.

Author contributions

- Adam Bajinting conceived, designed, performed, and analyzed experiments, wrote the paper, and reviewed drafts of the paper.
- Ho Leung Ng conceived, designed, and analyzed experiments, wrote the paper, reviewed drafts of the paper, and supervised the project.

REFERENCES

Bocharov EV., Lesovoy DM., Goncharuk SA., Goncharuk MV., Hristova K., Arseniev AS. 2013. Structure of FGFR3 Transmembrane Domain Dimer: Implications for Signaling and Human Pathologies. *Structure* 21:2087–2093. DOI: 10.1016/j.str.2013.08.026.

Brooks AN., Kilgour E., Smith PD. 2012. Molecular Pathways: Fibroblast Growth Factor Signaling: A New Therapeutic Opportunity in Cancer. *Clinical Cancer Research* 18:1855–1862. DOI: 10.1158/1078-0432.CCR-11-0699.

Daniele G., Corral J., Molife LR., Bono JS de. 2012. FGF Receptor Inhibitors: Role in Cancer Therapy. *Current Oncology Reports* 14:111–119. DOI: 10.1007/s11912-012-0225-0.

Dieci MV., Arnedos M., Andre F., Soria JC. 2013. Fibroblast Growth Factor Receptor Inhibitors as a Cancer Treatment: From a Biologic Rationale to Medical Perspectives. *Cancer Discovery* 3:264–279. DOI: 10.1158/2159-8290.CD-12-0362.

Kalinina J., Dutta K., Ilghari D., Beenken A., Goetz R., Eliseenkova AV., Cowburn D., Mohammadi M. 2012. The alternatively spliced acid box region plays a key role in FGF receptor autoinhibition. *Structure (London, England: 1993)* 20:77–88. DOI: 10.1016/j.str.2011.10.022.

Kapust RB., Waugh DS. 1999. Escherichia coli maltose-binding protein is uncommonly effective at promoting the solubility of polypeptides to which it is fused. *Protein Science: A Publication of the Protein Society* 8:1668–1674. DOI: 10.1110/ps.8.8.1668.

Klock HE., Lesley SA. 2009. The Polymerase Incomplete Primer Extension (PIPE) method applied to high-throughput cloning and site-directed mutagenesis. *Methods in Molecular Biology (Clifton, N.J.)* 498:91–103. DOI: 10.1007/978-1-59745-196-3_6.

Lemmon MA., Schlessinger J. 2010. Cell Signaling by Receptor Tyrosine Kinases. *Cell* 141:1117–1134. DOI: 10.1016/j.cell.2010.06.011.

Loll PJ. 2014. Membrane proteins, detergents and crystals: what is the state of the art? *Acta Crystallographica Section F Structural Biology Communications* 70:1576–1583. DOI: 10.1107/S2053230X14025035.

Mohammadi M., Schlessinger J., Hubbard SR. 1996. Structure of the FGF receptor tyrosine kinase domain reveals a novel autoinhibitory mechanism. *Cell* 86:577–587.

Patstone G., Maher P. 1996. Copper and calcium binding motifs in the extracellular domains of fibroblast growth factor receptors. *The Journal of Biological Chemistry* 271:3343–3346.

Pellegrini L., Burke DF., von Delft F., Mulloy B., Blundell TL. 2000. Crystal structure of fibroblast growth factor receptor ectodomain bound to ligand and heparin. *Nature* 407:1029–1034. DOI: 10.1038/35039551.

Plotnikov AN., Hubbard SR., Schlessinger J., Mohammadi M. 2000. Crystal structures of two FGF-FGFR complexes reveal the determinants of ligand-receptor specificity. *Cell* 101:413–424.

Plotnikov AN., Schlessinger J., Hubbard SR., Mohammadi M. 1999. Structural Basis for FGF Receptor Dimerization and Activation. *Cell* 98:641–650. DOI: 10.1016/S0092-8674(00)80051-3.

Privé GG. 2007. Detergents for the stabilization and crystallization of membrane proteins. *Methods* 41:388–397. DOI: 10.1016/j.ymeth.2007.01.007.

Sanchez-Heras E., Howell FV., Williams G., Doherty P. 2006. The fibroblast growth factor receptor acid box is essential for interactions with N-cadherin and all of the major isoforms of neural cell adhesion molecule. *The Journal of Biological Chemistry* 281:35208–35216. DOI: 10.1074/jbc.M608655200.

Schlessinger J., Plotnikov AN., Ibrahimi OA., Eliseenkova AV., Yeh BK., Yayon A., Linhardt RJ., Mohammadi M. 2000. Crystal Structure of a Ternary FGF-FGFR-Heparin Complex Reveals a Dual Role for Heparin in FGFR Binding and Dimerization. *Molecular Cell* 6:743–750. DOI: 10.1016/S1097-2765(00)00073-3.

Turner N., Grose R. 2010. Fibroblast growth factor signalling: from development to cancer. *Nature Reviews Cancer* 10:116–129. DOI: 10.1038/nrc2780.

Wang F., Kan M., Yan G., Xu J., McKeehan WL. 1995. Alternately spliced NH2-terminal immunoglobulin-like Loop I in the ectodomain of the fibroblast growth factor (FGF) receptor 1 lowers affinity for both heparin and FGF-1. *The Journal of Biological Chemistry* 270:10231–10235.

Yeh BK., Eliseenkova AV., Plotnikov AN., Green D., Pinnell J., Polat T., Gritli-Linde A., Linhardt RJ., Mohammadi M. 2002. Structural Basis for Activation of Fibroblast Growth Factor Signaling by Sucrose Octasulfate. *Molecular and Cellular Biology* 22:7184–7192. DOI: 10.1128/MCB.22.20.7184-7192.2002.

Yu K., Herr AB., Waksman G., Ornitz DM. 2000. Loss of fibroblast growth factor receptor 2 ligand-binding specificity in Apert syndrome. *Proceedings of the National Academy of Sciences of the United States of America* 97:14536–14541. DOI: 10.1073/pnas.97.26.14536.

Zhang F., Zhang Z., Lin X., Beenken A., Eliseenkova AV., Mohammadi M., Linhardt RJ. 2009. Compositional Analysis of Heparin/Heparan Sulfate Interacting with Fibroblast Growth Factor·Fibroblast Growth Factor Receptor Complexes. *Biochemistry* 48:8379–8386. DOI: 10.1021/bi9006379.